Driven Dissipative Majorana Dark Spaces

Matthias Gau,[1,2] Reinhold Egger,[1] Alex Zazunov,[1] and Yuval Gefen[2]
[1]Institut für Theoretische Physik, Heinrich-Heine-Universität, D-40225 Düsseldorf, Germany
[2]Department of Condensed Matter Physics, Weizmann Institute, Rehovot, Israel

(Received 30 March 2020; accepted 1 September 2020; published 1 October 2020)

Pure quantum states can be stabilized in open quantum systems subject to external driving forces and dissipation by environmental modes. We show that driven dissipative (DD) Majorana devices offer key advantages for stabilizing degenerate state manifolds ("dark spaces") and for manipulating states in dark spaces, both with respect to native (non-DD) Majorana devices and to DD platforms with topologically trivial building blocks. For two tunnel-coupled Majorana boxes, using otherwise only standard hardware elements (e.g., a noisy electromagnetic environment and quantum dots with driven tunnel links), we propose a dark qubit encoding. We anticipate exceptionally high fault tolerance levels due to a conspiracy of DD-based autonomous error correction and topology.

DOI: 10.1103/PhysRevLett.125.147701

Introduction.—Open quantum systems may be stabilized in a pure quantum state for arbitrarily long times by the interaction with an external driving field and a dissipative environment [1–13]. Such DD-stabilized dark states are eigenstates of the Lindbladian dissipator with zero eigenvalue when the system dynamics can be described by a Lindblad equation [14–18]. The latter is the most general Markovian master equation preserving the trace and semipositiveness of the density matrix. Using trapped ions or superconducting qubits, DD-stabilized dark states have recently been implemented experimentally [19–27]. For a stabilized manifold of multiple degenerate dark states (a dark space) [19,28–30], a robust quantum memory platform can be envisioned. Moreover, once states within a dark space can also be manipulated in a protected way, fault-tolerant quantum computing schemes without active feedback may become a viable option (see Refs. [31–38] for related work). At present, experimental studies of autonomous error correction in a DD qubit [25,27,39,40] report fidelities below 90% for state stabilization and significantly lower fidelity for gate operations.

In this Letter, we show that devices harboring Majorana bound states (MBSs) [41–53] provide a particularly attractive platform for the DD stabilization of degenerate dark spaces and for manipulating states in such spaces. The use of topologically protected building blocks for stabilizing DD dark spaces offers several key advantages for quantum state stabilization and manipulation protocols when compared to DD schemes with topologically trivial building blocks or to topological platforms without DD protection: (i) Majorana-based dark spaces benefit from both topological protection and DD-based autonomous error correction capabilities. In particular, the reduced intrinsic noise levels expected from the topological protection help to avoid unwanted residual dissipation effects within the dark space manifold [54]. (ii) As indicated in Fig. 1, our DD protocols exploit unidirectional cotunneling processes between pairs of quantum dots (QDs), which are connected by tunnel contacts to MBSs and by a driven tunnel link to each other. Dissipation here originates in a natural way from the electromagnetic environment. A weak driving field serves to pump electrons from QD 1 to the energetically high-lying QD 2 in Fig. 1, and the electron transfer from QD $2 \to 1$ then proceeds by inelastic cotunneling. By choosing predesignated tunnel couplings, this pumping-cotunneling cycle allows one to engineer at will jump operators acting on the Majorana state. Once a working Majorana platform becomes available, only standard hardware elements are needed to realize the proposed DD Majorana setups. (iii) The MBS-based dark space

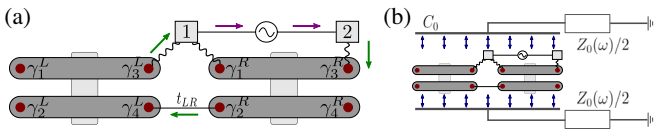

FIG. 1. Driven dissipative Majorana device with two tunnel-coupled Majorana boxes. (a) Each island harbors four Majorana states ($\gamma_\nu^{\kappa=L/R}$, red dots). The latter are shown as end states of topological hybrid nanowires (horizontal bars), which are connected by a superconducting bridge (vertical bar) to form a floating mesoscopic island [55,56]. Two quantum dots (boxes 1 and 2) are connected by tunnel contacts (wavy lines) to Majoranas. A driven tunnel link (solid line) connects both dots. The colored arrows illustrate the pumping-cotunneling cycle explained in the main text, stressing the nonlocal character of the processes involved. The shown trajectory amounts to the action of the operator $Z_L Y_R$ on the Majorana state [see Eq. (1)]. (b) Electromagnetic fluctuations of the surrounding electric circuit, modeled by the capacitance C_0 and the impedance $Z_0(\omega)$, cause inelastic tunneling processes.

stabilization is very robust with respect to variations of stabilization parameters. Deviations of up to ≈10% in these gate-tunable parameters are tolerable while retaining almost perfect fidelity. This remarkable degree of robustness is due to the spatial disentanglement of drive and dissipation processes (see Fig. 1), which in turn is connected to the nonlocality of the MBS system. (iv) State preparation and manipulation protocols within the dark space can be implemented in a flexible and rather simple manner.

We here illustrate these points for a device with two tunnel-coupled Majorana boxes [55,56] operated under Coulomb blockade conditions (see Fig. 1 for a schematic sketch). Each box harbors four MBSs. Our main results are as follows. We first show that over a wide parameter regime the dynamics in the Majorana sector is governed by a Lindblad equation, Eq. (5) below, which includes a Hamiltonian describing the unitary part of the time evolution and a Lindbladian dissipator responsible for the dissipative dynamics. Second, we demonstrate that this system can be engineered to support a multidimensional degenerate dark space. Third, to ensure that a generic initial state evolves toward a designated pure state within the dark space, one has to adiabatically break the degeneracy of the dark space during the intermediate stages of the protocol. We view this as a paradigmatic protocol (applicable to even more complex systems) for the preparation and manipulation of a state within a degenerate dark space, where we also explain how to optimize the speed of approach and the fidelity. Finally, we show how to manipulate states within the dark space. Our results are illustrated for a dark space that is equivalent to a fault-tolerant dark qubit. We note that in networks of coupled dark qubits, the active error correction required in Majorana surface code proposals [57–62] could become obsolete. Detailed derivations and specific state stabilization protocols are described in Ref. [63].

Model.—Consider the architecture in Fig. 1, where two Coulomb-blockaded topological superconductor islands ($\kappa = L/R$ for the left/right island) harbor in total eight MBSs with operators $\gamma_\nu^\kappa = (\gamma_\nu^\kappa)^\dagger$, where $\nu = 1, \ldots, 4$. They obey the anticommutation relations $\{\gamma_\nu^\kappa, \gamma_{\nu'}^{\kappa'}\} = 2\delta_{\nu\nu'}\delta_{\kappa\kappa'}$. We here assume that all MBSs are sufficiently far away from each other to represent zero-energy states. In addition, the relevant energy scales should be below the pairing gap Δ such that above-gap quasiparticles can be neglected. Each mesoscopic island in Fig. 1 has a large (and, for simplicity, equal) charging energy E_C and is operated under Coulomb valley conditions. At temperatures $T \ll E_C$, the charge on the island is then quantized on timescales $\delta t > 1/E_C$, implying a parity constraint for the Majorana sector of each box, $\gamma_1^\kappa\gamma_2^\kappa\gamma_3^\kappa\gamma_4^\kappa = \pm 1$ [56]. Since the charge is gapped out, the remaining twofold degeneracy of the ground state of each island corresponds to the presence of two Majorana qubits [56]. The respective Pauli operators are [64]

$$X_\kappa = i\gamma_1^\kappa\gamma_3^\kappa, \qquad Y_\kappa = i\gamma_3^\kappa\gamma_2^\kappa, \qquad Z_\kappa = i\gamma_1^\kappa\gamma_2^\kappa. \quad (1)$$

This nonlocal representation allows one to access all Pauli operators through electron cotunneling processes between pairs of tunnel-coupled QDs [55,56,59,60]. We also need a phase-coherent tunnel link between the boxes, $H_{LR} = it_{LR}\gamma_4^L\gamma_2^R$, with real-valued $t_{LR} > 0$.

The single-level QDs in Fig. 1, with electron annihilation operator d_j for the jth QD, are described by the dot Hamiltonian $H_d = \sum_{j=1,2}\epsilon_j d_j^\dagger d_j$, where the level energies $\epsilon_1 < \epsilon_2$ should satisfy $|\epsilon_j| \ll E_C, \Delta$. The QDs are connected by a driven tunnel link, which we model by $H_{\rm drive}(t) = 2A\cos(\omega_0 t)d_1^\dagger d_2 + \text{H.c.}$ [65] with drive amplitude A. The driving frequency ω_0 is tuned in resonance with the transition energy between the QD levels $\omega_0 = \epsilon_2 - \epsilon_1$. Since the Majorana boxes are operated under Coulomb valley conditions, the total occupancy $N_d = \sum_j d_j^\dagger d_j$ of the QDs is also conserved on timescales $\delta t > 1/E_C$ [66]. We study the case $N_d = 1$, where a single electron is shared by both QDs. Finally, inelastic tunneling processes connecting QDs with the respective MBSs in Fig. 1 are modeled by

$$H_{\rm tun} = t_0\sum_{j,\nu,\kappa}\lambda_{j,\nu\kappa}e^{-i\phi_\kappa}e^{i\theta_j}d_j^\dagger\gamma_\nu^\kappa + \text{H.c.}, \quad (2)$$

where the $e^{i\phi_\kappa}$ ($e^{-i\phi_\kappa}$) factors in Eq. (2) ensure that an electron charge is added to (subtracted from) the respective island in a tunneling process [67–69]. With the overall energy scale $t_0 \ll E_C$, the complex-valued parameters $\lambda_{j,\nu\kappa}$ with $|\lambda_{j,\nu\kappa}| \le 1$ encode the transparency of the tunnel contact between d_j and γ_ν^κ [70]. For the setup in Fig. 1, the only nonzero parameters are $\lambda_{1,3L}$, $\lambda_{1,1R}$, and $\lambda_{2,3R}$. The electromagnetic environment enters Eq. (2) through fluctuating phase operators θ_j, which cause dephasing on the respective QD [67,68,71,72]. For simplicity, these fluctuations are described by a single bosonic bath: $H_{\rm env} = \sum_m E_m b_m^\dagger b_m$, where $E_m > 0$ and $\theta_j = \sum_m g_{j,m}(b_m + b_m^\dagger)$ with couplings $g_{j,m}$. The phases θ_j appear below only via the combination $\theta = \theta_1 - \theta_2$, where we define a bath spectral density $\mathcal{J}(\omega) = \pi\sum_m (g_{1,m} - g_{2,m})^2 E_m^2\delta(\omega - E_m)$. We study the most relevant Ohmic case (see also Ref. [73]),

$$\mathcal{J}(\omega) = \alpha\omega e^{-\omega/\omega_c}, \quad (3)$$

where $\alpha = (e^2/2h)\text{Re}Z(\omega = 0)$ is a dimensionless system-bath coupling and frequencies above the scale ω_c are suppressed. Here $Z(\omega) = [Z_0^{-1}(\omega) + i\omega C_0]^{-1}$ is the dynamical impedance of the environment [see Fig. 1(b)], and we study the regime $\alpha < 1$. To avoid photon-assisted excitations of above-gap quasiparticles or higher-charge states on the islands, we demand $\omega_c \ll E_C, \Delta$. Non-Ohmic environments [17] can similarly be studied. However, for the sub-Ohmic case, the mapping to a Lindbladian master equation is problematic, while for the super-Ohmic case, dissipative gaps can become very small.

Lindblad equation.—We focus on the weakly driven regime defined by

$$\tilde{g}_0 \ll T \ll \omega_0, \qquad A \lesssim \tilde{g}_0, \qquad \tilde{g}_0 = t_0^2 t_{LR}/E_C^2, \quad (4)$$

where the energy scale $\tilde{g}_0$ characterizes the relevant cotunneling processes (see below). The driving-induced rate for pumping electrons between QDs 1 and 2 is thus assumed small against cotunneling rates. The condition $\tilde{g}_0 \ll T$ is needed to justify the Born-Markov approximation, while $T \ll \omega_0$ is required for the rotating wave approximation. Both approximations are used for deriving the Lindblad equation. Next, we switch to the interaction picture with respect to $H_d + H_{\rm env}$ and use third-order perturbation theory in the tunnel couplings to project the theory to the lowest-energy charge sector of each island. We then trace the von-Neumann equation over the bath and the QD degrees of freedom. As a result, the reduced density matrix $\rho_M(t)$ describing the Majorana sector obeys the Lindblad equation [63]

$$\partial_t \rho_M(t) = -i[H_L, \rho_M(t)] + \sum_{n=1,2} \Gamma_n \mathcal{L}[K_n]\rho_M(t), \quad (5)$$

where the dissipator $\mathcal{L}$ acts on ρ_M according to [17] $\mathcal{L}[K]\rho_M = K\rho_M K^\dagger - \frac{1}{2}\{K^\dagger K, \rho_M\}$. With $\lambda_{LR} \equiv t_{LR}/E_C \ll 1$ and the Pauli operators (1), we obtain the two jump operators in Eq. (5) as

$$K_1 = ie^{i\beta_2}|\lambda_{2,3R}|\left(e^{-i\beta_1}\frac{|\lambda_{1,1R}|}{\lambda_{LR}}X_R + i|\lambda_{1,3L}|Z_L Y_R\right) \quad (6)$$

and $K_2 = K_1^\dagger$, using the gauge choice $\lambda_{1,1R} = |\lambda_{1,1R}|e^{-i\beta_1}$, $\lambda_{1,3L} = |\lambda_{1,3L}|$, and $\lambda_{2,3R} = |\lambda_{2,3R}|e^{-i\beta_2}$. The coherent evolution in Eq. (5) is due to the Hamiltonian

$$H_L = 2p\tilde{g}_0 K_z + \sum_{n=1,2} h_n K_n^\dagger K_n,$$
$$K_z = \sin\beta_1 |\lambda_{1,1R}\lambda_{1,3L}| Z_L Z_R. \quad (7)$$

For the spectral density in Eq. (3), assuming $\omega_c \gg \omega_0$, the dissipative transition rates Γ_n and the Lamb shift parameters h_n are given by

$$\Gamma_1 = 2p\Gamma(1-2\alpha)\sin(2\pi\alpha)\left(\frac{\omega_0}{\omega_c}\right)^{2\alpha}\frac{\tilde{g}_0^2}{\omega_0},$$
$$\Gamma_2 = \frac{(1-p)}{2p}e^{-\omega_0/T}\Gamma_1,$$
$$h_1 = \frac{1}{2}\cot(2\pi\alpha)\Gamma_1, \qquad h_2 = \frac{(1-p)}{2p}e^{-\omega_0/T}h_1, \quad (8)$$

where $p \approx A/\omega_0$ is the steady-state occupation probability of the energetically high-lying QD 2, and $\Gamma(z)$ denotes the Gamma function.

At low temperatures $T \ll \omega_0$, the ratios Γ_2/Γ_1 and h_2/h_1 are exponentially small, and therefore only the jump operator K_1 is important. This operator can be traced back to *unidirectional* cotunneling transitions, where an electron is transferred from QD 2 to QD 1 by cotunneling through the double-box setup. In the steady state, a weak drive amplitude A is then responsible for pumping the dot electron back (from QD $1 \to 2$) via the driven tunnel link. We note that the parameters $A, \omega_0, \alpha, \omega_c$, and $\tilde{g}_0$ only affect the rates Γ_n and Lamb shifts h_n, which in turn determine the speed of approach toward the dark space. The dark space itself, however, will be determined by the choice of the jump operator K_1, which can be engineered by tuning the "state design parameters" $\lambda_{j,\nu\kappa}$ [see Eq. (6)]. These parameters can be adjusted via gate voltages. The ability to design jump operators via unidirectional cotunneling processes in such a manner is rooted in the nonlocal Majorana representation of the Pauli operators in Eq. (1), and thus in the underlying topological nature of our DD system.

Dissipative maps.—The key idea of our DD protocols is to choose the state design parameters $\lambda_{j,\nu\kappa}$ such that K_1 implements a selected dissipative map [10,12], which in turn directly drives $\rho_M(t)$ to the desired dark space. Below we use the four Bell states, $|\psi_\pm\rangle = (|00\rangle \pm |11\rangle)/\sqrt{2}$ and $|\phi_\pm\rangle = (|01\rangle \pm |10\rangle)/\sqrt{2}$, which are eigenstates of both $Z_L Z_R = \pm 1$ and $X_L X_R = \pm 1$ and span the Hilbert space of the two qubits in Eq. (1). We then define the dissipative maps $\hat{E}_{1,\pm} = (\mathbb{1} \pm Z_L Z_R)X_R$ (see Ref. [22]). In the Lindblad equation, a dissipative term $\propto \mathcal{L}[\hat{E}_{1,-}]\rho_M$ will map even-parity ($Z_L Z_R = +1$) states onto the respective odd-parity states, e.g., $\hat{E}_{1,-}|\psi_\pm\rangle = |\phi_\pm\rangle$. In contrast, odd-parity states do not evolve in time, $\hat{E}_{1,-}|\phi_\pm\rangle = 0$, and thus represent steady-state solutions. (Similarly, $\hat{E}_{1,+}$ maps odd-parity to even-parity states.) As is shown next, under the dissipative map $\hat{E}_{1,-}$, the system can then be driven into the degenerate odd-parity sector spanned by $|\phi_+\rangle$ and $|\phi_-\rangle$.

Dark space stabilization.—We now choose the parameters in Eq. (2) as

$$\beta_1 = \pi, \qquad |\lambda_{1,1R}| = \lambda_{LR}|\lambda_{1,3L}|, \quad (9)$$

with arbitrary $|\lambda_{2,3R}|$ and β_2. Inserting Eq. (9) into Eq. (6) shows that $K_1 \propto \hat{E}_{1,-}$. Moreover, from Eq. (7) we obtain $H_L \propto Z_L Z_R$. Since the dissipator in Eq. (5) only involves $K_1 \propto \hat{E}_{1,-}$ at $T \ll \omega_0$, the desired dissipative map can be realized without obstruction from the Hamiltonian dynamics. For this case, we can identify four conserved quantities (cf. Ref. [10]),

$$C_{1,\pm} = \frac{1}{2}(\mathbb{1} \pm Z_L), C_{2,\pm} = \frac{1}{2}(X_L \pm iY_L)X_R. \quad (10)$$

The basis of the matrix Hilbert space corresponding to the dark space [10] then follows as

$$M_{1,\pm} = \frac{1}{4}(\mathbb{1} \pm Z_L)(\mathbb{1} \mp Z_R),$$
$$M_{2,\pm} = \frac{1}{4}(X_L \pm iY_L)(X_R \mp iY_R). \tag{11}$$

The above DD protocol thus stabilizes a degenerate dark space of dimension $D = 4$ in the terminology of Refs. [10,12], which in turn coincides with the dark space dimension of a stabilized qubit space. The Pauli operators (X_D, Y_D, Z_D) for the resulting *dark Majorana qubit* can be chosen as

$$X_D = X_L X_R = -\gamma_1^L \gamma_3^L \gamma_1^R \gamma_3^R,$$
$$Y_D = Y_L X_R = \gamma_2^L \gamma_3^L \gamma_1^R \gamma_3^R, \qquad Z_D = Z_L = i\gamma_1^L \gamma_2^L. \tag{12}$$

The DD qubit encoding (12) is essential for fault tolerance, comparable to the formation of logical vs physical qubits in surface codes [74]. In our case, the DD protocol adds an extra protection layer on top of the topological protection of a native Majorana qubit. In particular, pure states will thereby be stabilized for indefinite time [75].

Approaching the dark space.—Starting from an arbitrary initial state $\rho_M(0)$, we monitor the approach toward a pure target state $|\Psi\rangle$ in terms of the fidelity $F(t) = \mathrm{tr}[|\Psi\rangle\langle\Psi|\rho_M(t)]$, where $\rho_M(t)$ is the solution of Eq. (5). During the time evolution, all symmetry properties of the initial state other than parity remain preserved. For example, starting with $\rho_M(0) = |\psi_+\rangle\langle\psi_+|$, since $X_L X_R = +1$ is kept as one approaches the target state, one finds $|\Psi\rangle = |\phi_+\rangle$ within the dark space. In Fig. 2, we show the fidelity obtained by the numerical integration of Eq. (5) for a maximally mixed initial state $\rho_M(0) = \frac{1}{4}\mathbb{1} \otimes \mathbb{1}$, where the corresponding target state is $|\Psi\rangle = (|\phi_+\rangle + |\phi_-\rangle)/\sqrt{2}$. We note that if the initial state is not precisely known, one can first stabilize an arbitrary state inside the dark space and subsequently drag that state toward the desired target state using the method described below. A convenient way to initialize the dark qubit is to employ the tunnel couplings to a third QD [63]. Figure 2 demonstrates that the dark-space fidelity is extremely robust against variations of the stabilization parameters $\lambda_{j,\nu\kappa}$. Even when allowing for "errors" of 20% in *all* these parameters, the fidelity is still $F \approx 0.9$. The timescale for approaching the steady state is given by the inverse of the *dissipative gap* Δ_{diss}, which is the smallest real part of the nonzero eigenvalues of the Lindbladian dissipator. For the above DD protocol, we obtain $\Delta_{\mathrm{diss}} \simeq |4\lambda_{1,3L}\lambda_{2,3R}|^2 \sum_n \Gamma_n$, resulting in $\Delta_{\mathrm{diss}}^{-1} \approx 3\ \mu s$ for the parameters in Fig. 2. Finally, methods for readout of the target state can be formulated as for the native Majorana qubit [55,56,63].

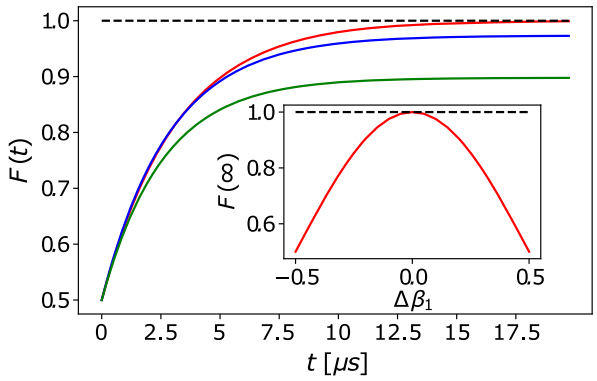

FIG. 2. Fidelity for approaching the dark space starting from a maximally mixed initial state. Main panel: Fidelity vs time, with $E_C = 1$ meV, $\tilde{g}_0/E_C = 10^{-4}$, $T/\tilde{g}_0 = 2$, $\omega_0/\tilde{g}_0 = 200$, $\omega_c/\tilde{g}_0 = 10^3$, $\alpha = 0.99$, $p(A) = 0.01$, and $|\lambda_{2,3L}| = 1$. The red curve is for ideal state design parameters [see Eq. (9)] with $|\lambda_{1,1R}| = 1$. The blue (green) curve is for parameters with a 10% (20%) deviation from their respective ideal values. Inset: Asymptotic ($t \to \infty$) fidelity vs percentage deviation $\Delta\beta_1$ from $\beta_1 = \pi$ with otherwise ideal parameters.

State manipulation.—We next discuss a general manipulation protocol moving an initial pure state in the dark space to an arbitrary final state in the dark space. We adiabatically switch on a perturbation breaking at least one conservation law in Eq. (10). The perturbation breaks the qubit degeneracy during the protocol, but once the perturbation is switched off, the degenerate dark space is fully stabilized again. The main challenges are to avoid coupling the dark space to other Hilbert space sectors that are not part of the decoherence-free subspace and to preserve the purity of the state. In particular, the drive should not connect odd- and even-parity sectors. It is convenient to break two conserved quantities at any given time, leaving a twofold degeneracy. The simplest protocol employs a "Z_L drive" realized by coupling γ_1^L and γ_2^L [see Eq. (12)]. We thus add a term $H_Z = iA_Z(t)\gamma_1^L\gamma_2^L = A_Z(t)Z_L$. The hybridization energy $A_Z(t)$ can be adiabatically changed using a gate-tunable tunnel link. H_Z commutes with $Z_L Z_R$ and thus conserves

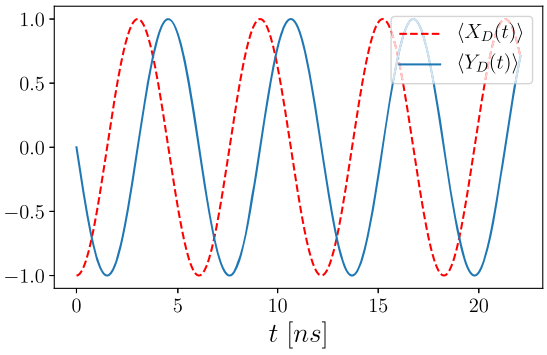

FIG. 3. State manipulation by a Z_L drive (see main text) with $A_Z/E_C = 10^{-4}$. We use the state design parameters in Eq. (9) and other parameters as in Fig. 2. The dynamics of the expectation values of the Pauli operators (12) reveals oscillatory qubit coherences. At all times, we numerically find $\langle Z_D\rangle = 0$ and, of course, $\langle Z_L Z_R\rangle = -1$ (odd parity).

parity. The evolution generated by H_Z therefore automatically remains in the odd-parity sector. Since $[H_Z, C_2] \neq 0$ and $[H_Z, C_3] \neq 0$ [see Eq. (10)], dark state coherences now depend on time. This is confirmed by our numerical results for constant A_Z in Fig. 3, where we start from $\rho_M(0) = |\phi_-\rangle\langle\phi_-|$ and find oscillations in the real part, $\langle X_D(t)\rangle = \langle X_L X_R\rangle(t)$, and the imaginary part, $\langle Y_D(t)\rangle = \langle Y_L X_R\rangle(t)$, of the coherences. In the Bloch vector representation, the dark state periodically rotates in the xy plane with oscillation period A_Z^{-1}, where $A_Z^{-1} \approx 6$ ns in Fig. 3. For a general adiabatic protocol $A_Z(t)$, it stands to reason that an arbitrary final state inside the dark space can be reached.

Conclusions.—We have introduced a DD Majorana platform for stabilizing a degenerate dark space that offers several key advantages. In particular, the spatial disentanglement of drive and dissipation processes rooted in the topological protection of MBSs allows for remarkably high levels of robustness. Future work should address the fidelity and purity during state manipulations and the high-dimensional dark spaces in DD systems with many coupled boxes.

We thank A. Altland, S. Diehl, and K. Snizhko for helpful discussions. This project has been funded by the Deutsche Forschungsgemeinschaft (DFG, German Research Foundation) under Grant No. 277101999, TRR 183 (project C01), under Germany's Excellence Strategy—Cluster of Excellence Matter and Light for Quantum Computing (ML4Q) EXC 2004/1—390534769, and under Grant No. EG 96/13-1. In addition, we acknowledge funding by the Israel Science Foundation.

[1] M. B. Plenio, S. F. Huelga, A. Beige, and P. L. Knight, Phys. Rev. A **59**, 2468 (1999).
[2] A. Beige, D. Braun, B. Tregenna, and P. L. Knight, Phys. Rev. Lett. **85**, 1762 (2000).
[3] M. B. Plenio and S. F. Huelga, Phys. Rev. Lett. **88**, 197901 (2002).
[4] S. Diehl, A. Micheli, A. Kantian, B. Kraus, H. P. Büchler, and P. Zoller, Nat. Phys. **4**, 878 (2008).
[5] B. Kraus, H. P. Büchler, S. Diehl, A. Kantian, A. Micheli, and P. Zoller, Phys. Rev. A **78**, 042307 (2008).
[6] S. Diehl, W. Yi, A. J. Daley, and P. Zoller, Phys. Rev. Lett. **105**, 227001 (2010).
[7] S. Diehl, E. Rico, M. A. Baranov, and P. Zoller, Nat. Phys. **7**, 971 (2011).
[8] C. E. Bardyn, M. A. Baranov, C. V. Kraus, E. Rico, A. İmamoğlu, P. Zoller, and S. Diehl, New. J. Phys. **15**, 085001 (2013).
[9] P. Zanardi and L. C. Venuti, Phys. Rev. Lett. **113**, 240406 (2014).
[10] V. V. Albert and L. Jiang, Phys. Rev. A **89**, 022118 (2014).
[11] K. Jacobs, X. Wang, and H. M. Wiseman, New J. Phys. **16**, 073036 (2014).
[12] V. V. Albert, B. Bradlyn, M. Fraas, and L. Jiang, Phys. Rev. X **6**, 041031 (2016).
[13] N. Goldman, J. C. Budich, and P. Zoller, Nat. Phys. **12**, 639 (2016).
[14] G. Lindblad, Commun. Math. Phys. **48**, 119 (1976).
[15] G. Lindblad, *Nonequilibrium Entropy and Irreversibility* (D. Reidel Pub. Co., Dordrecht, Netherlands, 1983).
[16] C. Gardiner and P. Zoller, *Quantum Noise: A Handbook of Markovian and Non-Markovian Quantum Stochastic Methods with Applications to Quantum Optics* (Springer Verlag, Heidelberg, 2004).
[17] H.-P. Breuer and F. Petruccione, *The Theory of Open Quantum Systems* (Oxford University Press, Oxford, 2006).
[18] H. M. Wiseman and G. J. Milburn, *Quantum Measurement and Control* (Cambridge University Press, Cambridge, England, 2010).
[19] S. Touzard, A. Grimm, Z. Leghtas, S. O. Mundhada, P. Reinhold, C. Axline, M. Reagor, K. Chou, J. Blumoff, K. M. Sliwa, S. Shankar, L. Frunzio, R. J. Schoelkopf, M. Mirrahimi, and M. H. Devoret, Phys. Rev. X **8**, 021005 (2018).
[20] K. Geerlings, Z. Leghtas, I. M. Pop, S. Shankar, L. Frunzio, R. J. Schoelkopf, M. Mirrahimi, and M. H. Devoret, Phys. Rev. Lett. **110**, 120501 (2013).
[21] Y. Lu, S. Chakram, N. Leung, N. Earnest, R. K. Naik, Z. Huang, P. Groszkowski, E. Kapit, J. Koch, and D. I. Schuster, Phys. Rev. Lett. **119**, 150502 (2017).
[22] J. T. Barreiro, M. Müller, P. Schindler, D. Nigg, T. Monz, M. Chwalla, M. Hennrich, C. F. Roos, P. Zoller, and R. Blatt, Nature (London) **470**, 486 (2011).
[23] P. Schindler, M. Müller, D. Nigg, J. T. Barreiro, E. A. Martinez, M. Hennrich, T. Monz, S. Diehl, P. Zoller, and R. Blatt, Nat. Phys. **9**, 361 (2013).
[24] S. Shankar, M. Hatdridge, Z. Leghtas, K. M. Sliwa, A. Narla, U. Vool, S. M. Girvin, L. Frunzio, M. Mirrahimi, and M. H. Devoret, Nature (London) **504**, 419 (2013).
[25] Z. Leghtas, U. Vool, S. Shankar, M. Hatridge, S. M. Girvin, M. H. Devoret, and M. Mirrahimi, Phys. Rev. A **88**, 023849 (2013).
[26] F. Reiter, D. Reeb, and A. S. Sørensen, Phys. Rev. Lett. **117**, 040501 (2016).
[27] Y. Liu, S. Shankar, N. Ofek, M. Hatridge, A. Narla, K. M. Sliwa, L. Frunzio, R. J. Schoelkopf, and M. H. Devoret, Phys. Rev. X **6**, 011022 (2016).
[28] F. Iemini, L. Mazza, D. Rossini, R. Fazio, and S. Diehl, Phys. Rev. Lett. **115**, 156402 (2015).
[29] F. Iemini, D. Rossini, R. Fazio, S. Diehl, and L. Mazza, Phys. Rev. B **93**, 115113 (2016).
[30] R. Santos, F. Iemini, A. Kamenev, and Y. Gefen, arXiv:2002.00237.
[31] F. Verstraete, M. M. Wolf, and J. I. Cirac, Nat. Phys. **5**, 633 (2009).
[32] K. Fujii, M. Negoro, N. Imoto, and M. Kitagawa, Phys. Rev. X **4**, 041039 (2014).
[33] B. M. Terhal, Rev. Mod. Phys. **87**, 307 (2015).
[34] J. Kerckhoff, H. I. Nurdin, D. S. Pavlichin, and H. Mabuchi, Phys. Rev. Lett. **105**, 040502 (2010).
[35] K. W. Murch, U. Vool, D. Zhou, S. J. Weber, S. M. Girvin, and I. Siddiqi, Phys. Rev. Lett. **109**, 183602 (2012).
[36] E. Kapit, J. T. Chalker, and S. H. Simon, Phys. Rev. A **91**, 062324 (2015).
[37] E. Kapit, Phys. Rev. Lett. **116**, 150501 (2016).

[38] M. Herold, M. J. Kastoryano, E. T. Campbell, and J. Eisert, New J. Phys. **19**, 063012 (2017).
[39] F. Reiter, A. S. Sørensen, P. Zoller, and C. A. Muschik, Nat. Commun. **8**, 1822 (2017).
[40] S. Puri, A. Grimm, P. Campagne-Ibarcq, A. Eickbusch, K. Noh, G. Roberts, L. Jiang, M. Mirrahimi, M. H. Devoret, and S. M. Girvin, Phys. Rev. X **9**, 041009 (2019).
[41] J. Alicea, Rep. Prog. Phys. **75**, 076501 (2012).
[42] M. Leijnse and K. Flensberg, Semicond. Sci. Technol. **27**, 124003 (2012).
[43] C. W. J. Beenakker, Annu. Rev. Condens. Matter Phys. **4**, 113 (2013).
[44] S. Das Sarma, M. Freedman, and C. Nayak, npj Quantum Inf. **1**, 15001 (2015).
[45] R. Aguado, Riv. Nuovo Cimento **40**, 523 (2017).
[46] R. M. Lutchyn, E. P. A. M. Bakkers, L. P. Kouwenhoven, P. Krogstrup, C. M. Marcus, and Y. Oreg, Nat. Rev. Mater. **3**, 52 (2018).
[47] H. Zhang, D. E. Liu, M. Wimmer, and L. P. Kouwenhoven, Nat. Commun. **10**, 5128 (2019).
[48] Q. Liu, C. Chen, T. Zhang, R. Peng, Y. J. Yan, Chen-Hao-Ping Wen, X. Lou, Y. L. Huang, J. P. Tian, X. L. Dong, G. W. Wang, W. C. Bao, Q. H. Wang, Z. P. Yin, Z. X. Zhao, and D. L. Feng, Phys. Rev. X **8**, 041056 (2018).
[49] P. Zhang, K. Yaji, T. Hashimoto, Y. Ota, T. Kondo, K. Okazaki, Z. Wang, J. Wen, G. D. Gu, H. Ding, and S. Shin, Science **360**, 182 (2018).
[50] D. Wang, L. Kong, P. Fan, H. Chen, S. Zhu, W. Liu, L. Cao, Y. Sun, S. Du, J. Schneeloch *et al.*, Science **362**, 333 (2018).
[51] E. Sajadi, T. Palomaki, Z. Fei, W. Zhao, P. Bement, C. Olsen, S. Luescher, X. Xu, J. A. Folk, and D. H. Cobden, Science **362**, 922 (2018).
[52] S. Ghatak, O. Breunig, F. Yang, Z. Wang, A. A. Taskin, and Y. Ando, Nano Lett. **18**, 5124 (2018).
[53] A. Murani, B. Dassonneville, A. Kasumov, J. Basset, M. Ferrier, R. Deblock, S. Guéron, and H. Bouchiat, Phys. Rev. Lett. **122**, 076802 (2019).
[54] P. Facchi, V. Gorini, G. Marmo, S. Pascazio, and E. C. G. Sudarshan, Phys. Lett. A **275**, 12 (2000).
[55] S. Plugge, A. Rasmussen, R. Egger, and K. Flensberg, New J. Phys. **19**, 012001 (2017).
[56] T. Karzig, C. Knapp, R. M. Lutchyn, P. Bonderson, M. B. Hastings, C. Nayak, J. Alicea, K. Flensberg, S. Plugge, Y. Oreg, C. M. Marcus, and M. H. Freedman, Phys. Rev. B **95**, 235305 (2017).
[57] B. M. Terhal, F. Hassler, and D. P. DiVincenzo, Phys. Rev. Lett. **108**, 260504 (2012).
[58] S. Vijay, T. H. Hsieh, and L. Fu, Phys. Rev. X **5**, 041038 (2015).
[59] L. A. Landau, S. Plugge, E. Sela, A. Altland, S. M. Albrecht, and R. Egger, Phys. Rev. Lett. **116**, 050501 (2016).
[60] S. Plugge, L. A. Landau, E. Sela, A. Altland, K. Flensberg, and R. Egger, Phys. Rev. B **94**, 174514 (2016).
[61] D. Litinski, M. S. Kesselring, J. Eisert, and F. von Oppen, Phys. Rev. X **7**, 031048 (2017).
[62] C. Wille, R. Egger, J. Eisert, and A. Altland, Phys. Rev. B **99**, 115117 (2019).
[63] M. Gau, R. Egger, A. Zazunov, and Y. Gefen, companion paper, Phys. Rev. B **102**, 134501 (2020).
[64] B. Béri and N. R. Cooper, Phys. Rev. Lett. **109**, 156803 (2012).
[65] G. Platero and R. Aguado, Phys. Rep. **395**, 1 (2004).
[66] A. Romito and Y. Gefen, Phys. Rev. B **90**, 085417 (2014).
[67] M. H. Devoret, D. Esteve, H. Grabert, G.-L. Ingold, H. Pothier, and C. Urbina, Phys. Rev. Lett. **64**, 1824 (1990).
[68] S. M. Girvin, L. I. Glazman, M. Jonson, D. R. Penn, and M. D. Stiles, Phys. Rev. Lett. **64**, 3183 (1990).
[69] L. Fu, Phys. Rev. Lett. **104**, 056402 (2010).
[70] A. Zazunov, R. Egger, and A. Levy Yeyati, Phys. Rev. B **94**, 014502 (2016).
[71] Yu. V. Nazarov and Ya. M. Blanter, *Quantum Transport: Introduction to Nanoscience* (Cambridge University Press, Cambridge, England, 2010).
[72] A. Altland and B. D. Simons, *Condensed Matter Field Theory*, 2nd ed. (Cambridge University Press, Cambridge, England, 2010).
[73] M. I. K. Munk, R. Egger, and K. Flensberg, Phys. Rev. B **99**, 155419 (2019).
[74] A. G. Fowler, M. Mariantoni, J. M. Martinis, and A. N. Cleland, Phys. Rev. A **86**, 032324 (2012).
[75] Our DD scheme does not provide protection against quasiparticle poisoning beyond the protection mechanisms discussed in Refs. [55,56,60].